An-Najah University Journal for Research – A
Natural Sciences

Asymmetric Dual Air-Gap FR-4 Microstrip Patch Antenna for Surface-Wave Suppression and High-Efficiency Dual-Band Operation

Sarah Kareem Mohammed[1], Muayyed Jabar Zoory [2]*

Type: Full Article. Received: 20th May 2026, Accepted: 29th June 2026

Accepted Manuscript, In Press

Abstract A low-cost FR-4 microstrip patch antenna with high realized gain and radiation efficiency is presented in this paper using a novel asymmetric dual air-gap stack to effectively reduce dielectric loss and suppress surface-wave excitation. Beginning from a traditional FR-4 patch foundation, the configuration is developed through symmetrical and then asymmetrical air-gap integration in which both gaps enable additional design freedom to tune the resultant effective permittivity and coupling to parasitic patch. Full-wave simulations (CST) indicate that the gain of the prototype configuration reaches a maximum realized gain as high as 9.05 dB and the radiation efficiency is 83.1% compared with 2.29 dB and 36.5% for the template FR-4 design, respectively. The optimized air-gap spacing enables dual-band operation at 4.953 GHz and 8.146 GHz, with an impedance bandwidth of 526 MHz at the upper band. Surface-current distributions allude to the diminished surface-wave activity and enhanced radiation property of the investigated configuration. Because of its straightforward stack-up and use of standard FR-4, the antenna provides a pragmatic pathway to high-efficiency operation for sub-6 GHz and X-band wireless applications.

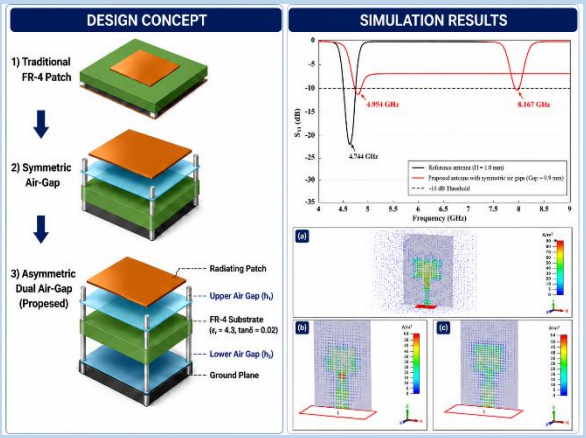

Keywords: Microstrip patch antenna; Asymmetric dual air-gap; High-efficiency antenna; Sub-6 GHz 5G; Energy-efficient wireless communications; Surface-wave suppression.

Introduction

With the growing deployment of fifth-generation (5G) wireless communication systems, as well as new low-band and X-band applications, there is an increasing need for multifunctional antenna solutions that can offer miniaturization, light weight, and high efficiency across multiple frequency bands(1-4). Among different antenna technologies, microstrip patch antennas (MPAs) have become very attractive due to their low profile, planar structure and low fabrication cost, as well as their simplicity to integrate with microwave circuits(5, 6). But unfortunately, conventional microstrip antennas are proposed to have limited bandwidth and moderate gain and low radiation efficiency when using a low-cost substrate like FR-4 for fabrication(7, 8).

The FR-4 substrates are the most commonly used in practical wireless systems because of low cost and availability; however, their relatively high dielectric loss tangent ($\tan\delta \approx 0.02$) has greatly hindered radiation efficiency and gain(9). Moreover, high-dielectric-constant substrates lead to surface-wave excitation, resulting in power confinement within the dielectric layer and increased power loss at the substrate edges(10, 11). These limitations prevent direct use of FR-4 in high-performance 5G and C-/X-band systems unless structural changes are made to reduce dielectric and surface-wave losses.

In recent years, many gain-enhancement and bandwidth-improvement techniques have been proposed to solve these issues. Mutations in the ground structures (DGS) are frequently used to change current distribution and surface waves, allowing for moderate gain and bandwidth increase(12, 13). Metasurface-based superstrates and partially reflective surfaces have emerged as alternatives that can yield significant gain improvement through controlling the phase distribution and collimating the electromagnetic fields(14, 15). Although these methods can provide enhancements beyond 9–10 dB, they typically involve either periodic structures, multi-layer constructs

[1] Department of Physics, College of Science, Mustansiriyah University, Baghdad, Iraq.
E-mail: Saracool1991@uomustansiriyah.edu.iq
[2] Department of Physics, College of Science, Mustansiriyah University, Baghdad, Iraq.
* Corresponding author: muayyedjz@uomustansiriyah.edu.iq
ORCID (Muayyed Jabar Zoory): https://orcid.org/0000-0002-5011-4618

or extra dielectric loadings, which add to structural complexity and manufacturing cost.

Another approach is to employ air-gap techniques, which offer an efficient and relatively simple method of reducing effective permittivity and lowering dielectric losses(16-18). To reduce the effective dielectric constant, an air layer is incorporated either in or above the substrate(19). which would improve fringing fields and radiation efficiency while suppressing surface-wave modes. Symmetric air-gap arrangements and layered patch structures have been studied to enhance antenna gain and bandwidth, but they often provide limited control of multi-resonance response, along with impedance-bandwidth adjustment(20).

However, only a few studies have investigated asymmetric dual air-gap configurations to independently control the effective permittivity and electromagnetic coupling between the radiating and parasitic elements, particularly when using low-cost FR-4 substrates. The asymmetric configuration presents additional degrees of freedom for tuning the resonance frequencies, surface-current distributions, and impedance characteristics independent of complex metasurfaces or reconfigurable circuits.

Based on this motivation, the present article proposes a high-efficiency FR-4 microstrip patch antenna with an asymmetric dual air-gap stack that simultaneously suppresses the surface wave and dielectric loading while improving the electromagnetic coupling. With a realizable gain of 9.05 dB and radiation efficiency higher than 83.1%, the structure combines simplicity in fabrication with metasurface-based or multilayer dielectric superstrate designs. Also, dual-band performance at 4.953 GHz and 8.146 GHz is obtained by tuning the heights of the lower and upper air gaps independently. The proposed scheme offers a practical and low-cost solution for high-performance wireless applications operating in the sub-6 GHz and X-band frequency bands.

Antenna Design and Geometry

This section discusses the geometry, material selection, and design methodology of the proposed asymmetric dual air-gap integrated microstrip patch antenna. Overall, the design aims to improve radiation efficiency and gain while maintaining a low-cost, fabrication-friendly structure based on a standard FR-4 substrate.

Antenna Structure and Material

The proposed antenna consists of a three-layer stacked-patch structure incorporating an FR-4 substrate and asymmetric dual air-gap layers. The configuration is optimized for dual-band operation in the sub-6 GHz and X-band frequency ranges while providing enhanced radiation performance. It is composed of a ground plane, an FR-4 dielectric substrate and two air gaps between parasitic metallic patch. The overall architecture is depicted in Fig. 1.

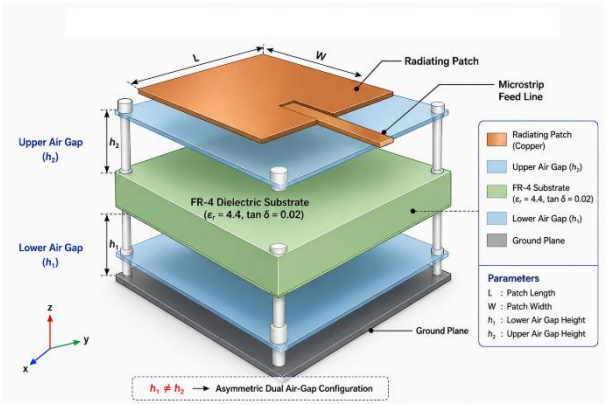

Figure 1: 3D geometry of the high-gain antenna with dual symmetric/asymmetric air gaps.

Specifically, the FR-4 substrate is used, with ϵ_r= 4.3 and tanδ = 0.02 due to its low cost and availability. Despite this, FR-4's high dielectric loss confines radiation efficiency and gain. To overcome this drawback, two air-gap layers (εr ≈ 1) are embedded above and below the dielectric substrate to lower the effective permittivity of the structure and mitigate the surface-wave propagation.

The ground plane and the first air gap form the bottom layer, whereas the FR-4 substrate with a radiating patch is in the middle layer. The upper layer also contains the second air gap and a parasitic patch element designed to improve electromagnetic coupling between radiating elements of the antenna and support multi-resonance behavior.

Feeding Technique and Impedance Matching

A microstrip line feed printed on the FR-4 substrate creates an excitation in the antenna. Using standard transmission line equations, the feedline is configured to have a characteristic impedance of 50 Ω. An inset-fed configuration is employed, which enhances impedance matching between the feedline and radiating patch.

We tune the inset depth and feedline width to optimize reflection coefficient (S11) at certain operating frequencies. The antenna presents S11 < −10 dB at both resonant frequencies due to optimizing parameters, which facilitates efficient power transfer and decreases mismatch losses.

Asymmetric Dual Air -Gap Configuration

The design refers to the above-mentioned important innovation, namely the asymmetric dual air-gap configuration. In contrast to traditional symmetric air-gap configurations, a second air gap with a different height enables more degrees of freedom in manipulating the antenna's electromagnetic response.

Specifically, the lower air gap mostly lowers its effective dielectric constant and also suspends surface-wave excitation from the lossy the FR-4 substrate. In contrast, the upper air gap is a parameter that determines the coupling between the radiating patch and the parasitic element, thus allowing adjustments to both resonance frequencies and bandwidth.

The asymmetry enables independent radiation efficiency, gain, and impedance bandwidth. Consequently, dual-band operation is obtained with a compact and low-complexity structure.

Design Evolution (Optimization Process)

First, the performance of the antenna in terms of gain, efficiency and bandwidth is studied.

Stage II: The second stage allows the introduction of symmetric air gaps that reduce dielectric loading, thus broadening radiation. While this setup offers a considerable increase in performance, it comes with poor control over several resonant modes.

Eventually, an asymmetric dual air-gap configuration is realized to independently optimize both the two heights of air gaps. This paves the way for a refined design of permittivity and electromagnetic coupling, leading to enhanced gain, wider operational bandwidth and dual-band operation as in Fig. 2.

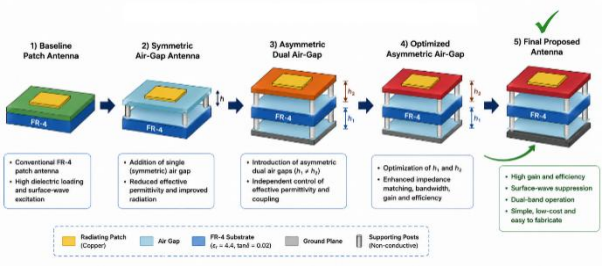

Figure 2: Design evolution of the proposed antenna from a conventional FR-4 patch to the asymmetric dual air-gap configuration.

Table 1 summarizes the final optimized dimensions of the proposed antenna. The optimization process was carried out through an iterative parametric analysis using CST Microwave Studio, as illustrated in Fig. 2.

The final antenna dimensions listed in Table 1 were obtained through a systematic optimization process. The air-gap layers were introduced progressively into the conventional microstrip patch antenna to improve its electromagnetic performance. Figure 3 illustrates the iterative simulation and optimization procedure implemented in CST Microwave Studio to achieve the maximum realized gain of 9.05 dB.

Table 1: Optimized dimensions of the proposed asymmetric dual air-gap antenna.

Parameters	Value (mm)
Resonance frequency	**5**
Substrate constant	**4.3**
Thickness of substrate h	h_{sub}
Width of patch wp	**18.43**
Length of patch lp	**14.2**
Width of ground wg	**33.6**
Length of ground lg	**62.24**
Width of substrate ws	**33.6**
Length of substrate ls	**162.24**
Width of feedline wf	**1.945**
Length of feedline	**13.833**
Edge feed width	**0.47**
Edge feed length	**8.703**
First air-gap height	h_{air1}
Second air-gap height	h_{air2}

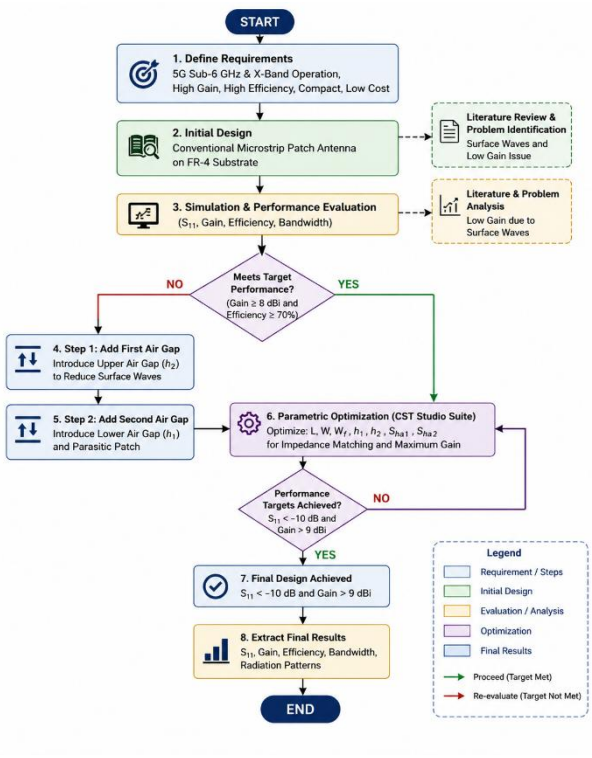

Figure 3: Flow chart of the proposed antenna design and optimization process.

Theoretical Analysis and Methodology

In this section, the performance improvement of the proposed antenna is explained theoretically. The improvements in gain, radiation efficiency, and impedance bandwidth are attributed to three main mechanisms: effective permittivity reduction, surface-wave suppression, and enhanced electromagnetic coupling introduced by the asymmetric dual air-gap structure.

Effective Permittivity Reduction Model

The addition of air-gap layers greatly alters the electromagnetic characteristics of the composite structure. The antenna is modelled as a multilayer dielectric system made up of the FR-4 substrate and two air layers. We can use an approximate series capacitance model for the effective permittivity of this structure, with each layer contributing to the total capacitance(21).

The effective permittivity can therefore be expressed as:

$$\frac{1}{C_{eq}} = \frac{h_1}{\varepsilon_0 A} + \frac{h_2}{\varepsilon_r \varepsilon_0 A} + \frac{h_3}{\varepsilon_0 A} \qquad (1)$$

$$\varepsilon_{eff} = \frac{(h_1 + h_2 + h_3)}{\left(h_1 + \frac{h_2}{\varepsilon_r} + h_3\right)} \qquad (2)$$

Where C_eq is the equivalent capacitance of the multilayer air–dielectric–air structure, ε_r is the relative permittivity of the FR-4 substrate and A is the effective overlapping area between conductive layers (m²). where (h_1), (h_2) and (h_3) define the thicknesses of the lower air gap, dielectric substrate, and upper

air gap, respectively, while (ε_r) is the relative permittivity of the FR-4 substrate.

Due to the dielectric constant of air being one, air gaps reduce overall permittivity. This minimization enhances the radiation efficiency and gain by causing more prominent fringing fields around the patch edges(1).

The effect of the effective permittivity on the resonance frequency of the antenna can be expressed in a well-known form for microstrip patch antennas:

$$f_r = \frac{c}{2L_{eff}\sqrt{\varepsilon_{eff}}} \qquad (3)$$

With f_rbeing the resonant frequency, c is the speed of light in free space, L_eff is the effective electrical length of the patch and ε_eff is the effective dielectric constant.

According to Eq. (3), the resonant frequency is inversely proportional to the square root of effective permittivity. Consequently, air-gap layers lower εeff and change the electromagnetic field distribution around the patch. This mechanism enables additional tuning flexibility of the resonant frequencies along with a simultaneous increase of radiation efficiency and suppression of surface-wave propagation.

Surface Wave Suppression Mechanism I

Microstrip antennas working on high-permittivity substrates like FR-4 will hold more than the 70% of electromagnetic energy trapped in their substrate in the state of surface waves. These waves travel at the substrate-air interface and eventually dissipate at the edges, resulting in a low radiation efficiency and distorted radiation patterns(1).

The power coupled to surface waves is highly sensitive to the substrate permittivity. Surface-wave modes can be suppressed by increasing their cutoff frequency while reducing the effective permittivity with layers of air-gap substrates(22).

This mechanism allows a greater portion of the input power to radiate into free space rather than remaining confined as surface-wave energy within the substrate. which is naturally confined within the substrate. This phenomenon is the reason for the improvement of radiation efficiency from 36.5% to more than 83.1% observed in the proposed design(23)

Asymmetry and Bandwidth Enhancement

Just a single air gap limits the degrees of freedom in adjusting the antenna electromagnetic performance. Unlike symmetric air-gap structures, in which both air gaps have identical heights, the proposed design employs different air-gap heights to provide additional optimization flexibility.

The impedance bandwidth is inversely proportional to the quality factor (Q-factor) in microstrip antennas, according to $(\mathrm{BW} \propto \frac{1}{Q})$(22).

A further increase of the effective height of the antenna reduces the Q-factor, thereby enhancing a bandwidth. The differential air-gap configuration shows that the cavity-shaped coupling mechanism could be selectively tuned while increasing the antenna height in total(1).

The main influence of the lower air gap is on effective permittivity and radiation efficiency, whereas the upper air gap dictates the electromagnetic coupling between the main radiating patch and parasitic element. Such interaction results in the establishment of two separate resonant modes, allowing for dual-band operations.

All these effects jointly yield a higher impedance bandwidth and cause a second resonance to appear at higher frequencies.

Equivalent Circuit Model Analysis

An equivalent circuit model (ECM) is also developed to verify the electromagnetic characteristics of the proposed antenna. At resonance, the antenna may be modelled by a parallel RLC resonator, where the input impedance is(1):

$$Z_{in} = \frac{1}{\frac{1}{R} + \frac{1}{jwL} + JwC} \qquad (4)$$

Where Z_{in} is the input impedance of the equivalent resonant circuit (Ω), (R) corresponding to the radiation resistance, (L) equivalent inductance (H), and (C) equivalent capacitance of the resonant circuit (F); w is the angular frequency (rad/s), defined as ω = 2πf; and Jis the imaginary unit, where j = √(-1) and f is the operating frequency (Hz).

Introducing air-gap layers reduces the effective capacitance, shifts the resonant frequency, and increases the impedance bandwidth. And the asymmetric configuration changes the coupling among resonant elements to provide multiple paths toward resonance.

As illustrated in Fig. 4, the equivalent circuit model (ECM) is built up for further interpretation of the electromagnetic behavior of this antenna. Fig. 4, where the antenna is treated as a parallel RLC resonator at its resonance frequency, and radiation resistance, inductance and capacitance show the first important electromagnetic features of the structure.

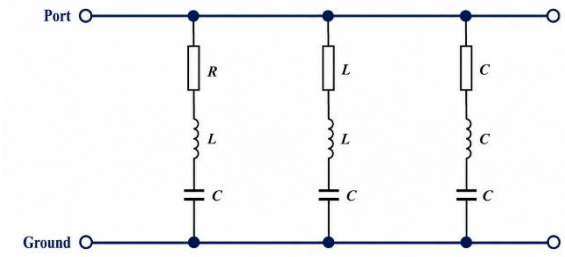

Figure 4: Equivalent circuit model (ECM) of the proposed antenna, represented by a parallel RLC resonator.

The equivalent circuit parameters corresponding to the fundamental resonance frequency were extracted from the CST simulation results. An agreement between the circuit model and full-wave simulation confirms a successful implementation of the proposed design approach.

Results and Discussion

In this section, a complete characterization of the proposed antenna has been performed by means of full-wave simulations using CST Microwave Studio. The outcomes are presented in a step-by-step design evolution, beginning from a conventional FR-4-based antenna configuration to symmetric and asymmetric dual air-gap designs.

The performance will be analyzed with respect to resonance behaviour, impedance matching, gain, radiation efficiency, bandwidth, and surface current distribution. The results are consistent with the theoretical analysis and simulation framework proposed in this study.

Conventional Antenna Design (Baseline) Performance

The basic design is a standard microstrip patch antenna produced on the FR-4 substrate. Since FR-4 has both a relatively high dielectric constant and loss tangent, the radiation performance of the antenna will be limited(1).

As shown in Table 2, the increase of substrate thickness (H) from 1.0 mm to 1.9 mm induces a shift in the resonance frequency from approximately 4.744 GHz to nearly 4.576 GHz gradually. This may be ascribed to the effective permittivity increase and improved fringing field effects.

Table 2: Impact of Substrate Thickness on Antenna Performance

H (mm)	Frequency (GHz)	VSWR	Gain (dBi)	S11 (dB)	Efficiency (%)	Bandwidth	Impedance (Ω)
1.0	4.744	1.215	2.29	20.26	36.5	0.11637	50
1.1	4.709	1.141	3.38	23.65	36.6	0.1257	51
1.2	4.695	1.114	3.38	25.39	38.2	0.13162	53.3
1.3	4.681	1.101	3.38	26.38	39.6	0.13818	56
1.4	4.660	1.087	3.36	27.56	41	0.14386	58.1
1.5	4.646	1.108	3.35	28.62	42.3	0.14794	60
1.6	4.625	1.074	3.32	28.91	43.5	0.15301	62
1.7	4.611	1.072	3.30	30.32	44.6	0.15927	64
1.8	4.597	1.063	3.28	30.24	45.5	0.16642	66
1.9	4.576	1.059	3.23	30.81	46.6	0.17222	67

Figure 5 illustrates the variation in realized gain with substrate thickness. The gain initially increases as the substrate thickness increases and then gradually reaches a saturation level. This configuration provides a maximum gain of ~3.38 dBi.

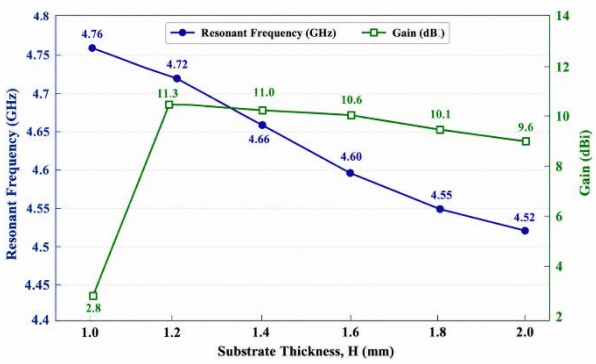

Figure 5: shows the resonant frequency vs. antenna gain dependent on the substrate thickness (H) for the basic microstrip antenna.

As shown in Table 2, the radiation efficiency remains relatively low (36.5–46.6%) despite the increase in substrate thickness. This behavior is primarily attributed to dielectric losses and the excitation of surface waves within the substrate.

These findings demonstrate that modifying the substrate thickness alone is insufficient to achieve high radiation performance, thereby justifying the introduction of the proposed air-gap structure.

Effect of Symmetric Air-Gap Configuration

Symmetric air gaps (above and below the FR-4 substrate) are therefore added to facilitate performance improvement over the baseline design. This modification reduces the effective permittivity of the antenna structure, resulting in improved radiation characteristics, as discussed in Section 3.1, resulting in improved radiation performance.

Fig. 6 shows the impact of air-gap thickness on antenna gain, representing a substantial improvement over the baseline design. the realized gain increases to approximately 8.76 dBi, representing more than a twofold improvement over the baseline design.

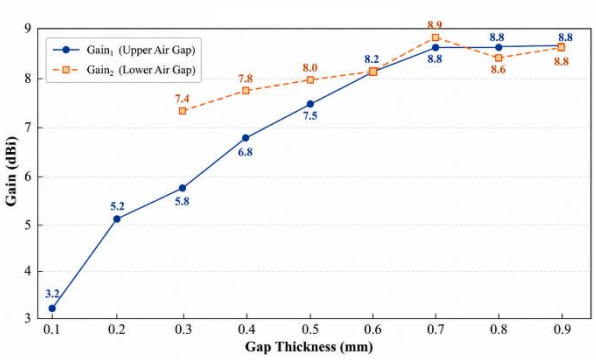

Figure 6: Gain vs air-gap thickness

Figure 7 shows that the introduction of the air-gap structure modifies the resonance characteristics, leading to the emergence of a second resonant frequency and enabling dual-band operation. As can be seen, when the thickness of the air gap is optimized to 0.9 mm, both resonances are obtained at approximately 4.954 GHz and 8.167 GHz, respectively.

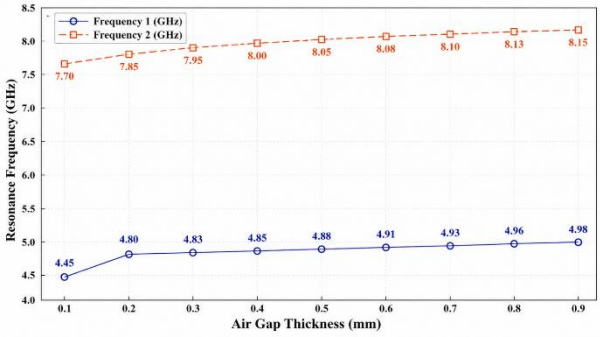

Figure 7: Resonant frequencies vs air-gap thickness

Fig. 8 shows the impedance matching performance, and the reflection coefficient (S_11) is always minimized to below −10 dB within the two frequency bands, indicating sufficient power transfer. In addition, a significant enhancement of the radiation efficiency is represented as about 83.7%. This improvement is in agreement with the theoretical expectation that a lower effective permittivity reduces surface-wave emission, thus enhancing radiation performance.

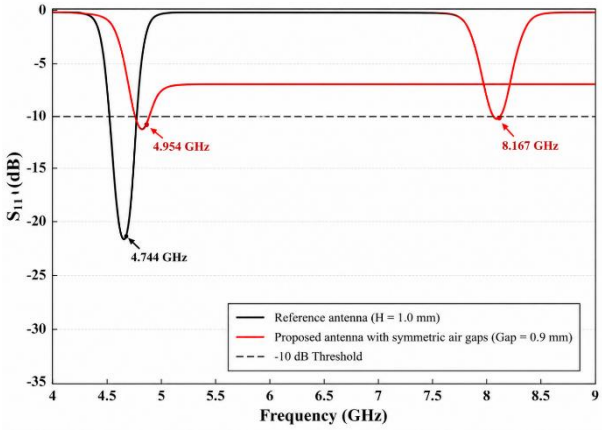

Figure 8: Simulated realized gain as a function of frequency for different asymmetric air-gap configurations.

Performance of the Asymmetric Dual Air-Gap Configuration

To improve the antenna performance, a further design parameter is introduced in terms of an asymmetric dual air gap, with the lower one fixed at 0.9 mm and the upper gap chosen to fit optimized electromagnetic characteristics. The descriptive performance characteristics are shown in Table 3.

Table 3. Performance analysis of the proposed antenna with a fixed first air-gap height of 0.9 mm and a variable second air-gap height.

Variable Gap (mm)	Total H (mm)	Band	Frequency (GHz)	VSWR	Gain (dBi)	S11 (dB)	Efficiency (%)	Bandwidth (GHz)
0.1	2.0	**f1**	4.457	1.647	6.88	12.24	70	0.11993
		f2	7.236	1.322	7.61	17.17	75	0.31472
0.2	2.1	**f1**	4.744	1.648	7.75	12.23	78.3	0.16108
		f2	7.782	1.553	8.09	13.29	81.7	0.34733
0.3	2.2	**f1**	4.786	1.664	8.18	12.06	79	0.167
		f2	7.880	1.638	8.20	12.33	82.2	0.34828
0.4	2.3	**f1**	4.828	1.685	8.50	11.87	80.7	0.23398
		f2	7.957	1.697	8.30	11.76	82.6	0.47367
0.5	2.4	**f1**	4.856	1.702	8.68	11.71	81.4	0.23958
		f2	8.013	1.747	8.42	11.31	82.8	0.48273
0.6	2.5	**f1**	4.919	1.712	8.71	11.61	82.1	0.25455
		f2	8.055	1.710	8.50	11.04	84.5	0.51834
0.7	2.6	**f1**	4.905	1.373	8.75	11.43	82.3	0.25793

		f2	8.097	1.780	8.59	11.04	83.6	0.51676
0.8	2.7	**f1**	4.933	1.735	8.75	11.41	83.1	0.26985
		f2	8.132	1.795	8.66	10.92	84.1	0.52602
0.9	2.8	**f1**	4.954	1.761	9.05	11.19	83.1	0.26985
		f2	8.146	1.839	8.60	10.59	83.9	0.52602

The results clearly demonstrate that the asymmetric dual air-gap configuration provides superior control over the resonance characteristics, realized gain, and impedance bandwidth compared with both the baseline and symmetric designs. This improvement is attributed to the additional design flexibility provided by independently optimizing the two air-gap heights.

As illustrated in Figure 9, the realized gain increases with the upper air-gap height and reaches a maximum value of 9.05 dBi at 4.954 GHz when the upper air-gap height is 0.9 mm. This improvement stems from the decrease in effective permittivity (ε_eff) and a favourable electromagnetic coupling between the radiating patch and parasitic component. This ε_eff minimizes fringing fields, which means better radiation efficiency and larger effective aperture.

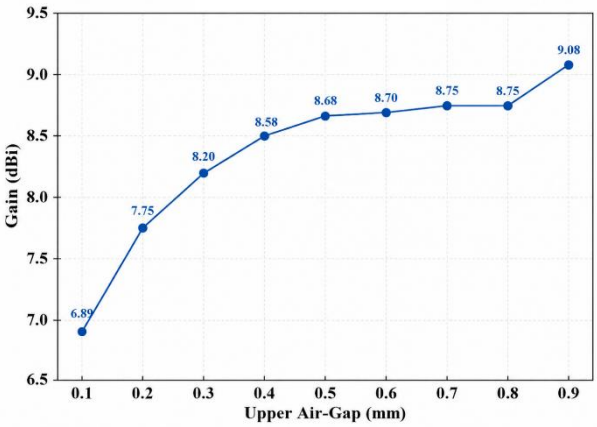

Figure 9: Variation of realized gain as a function of the upper air-gap height.

In addition, the upper air gap has a considerable effect on the resonance characteristics of this antenna. As shown in Figure 10, the fundamental resonant frequency (f_1) gradually shifts toward higher frequencies as the upper air-gap height increases with increasing air-gap height, and another resonance (f_2) appeared at about 8.146 GHz and became stable. The dual-band operation due to the asymmetric configuration has been confirmed by the excitation of more than one resonant mode for the controlled incidence angle.

These results show an increased bandwidth, especially at the upper band (≈526 MHz), which can be attributed to a lower antenna quality factor (Q-factor). This concurrent increase of the effective structure height reduces the stored reactive energy, allowing for increased impedance bandwidth. This behavior is supported by the theoretical analysis presented in this study.

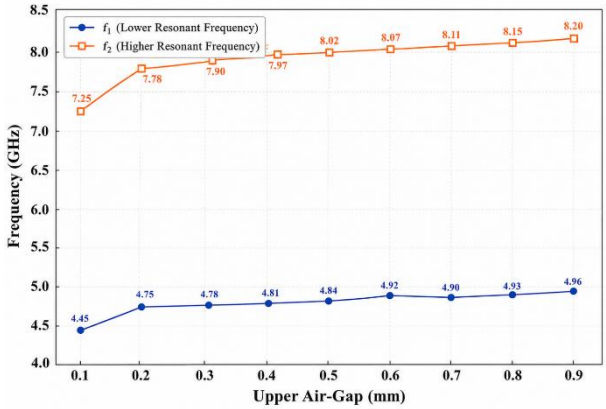

Figure 10: Variation of resonance frequencies (f_1 and f_2) with respect to the upper air-gap height.

As illustrated in Fig. 11, the impedance matching performance is assessed based on the reflection coefficient. As seen from the results, for both of the operating bands, $|S_{11}| < -10$ dB is also satisfied, while the VSWR remains below 1.8 at both operating frequencies, meaning impedance matching and power transfer efficiency at an acceptance level.

In addition, there is a significant improvement in the radiating efficiency with respect to this baseline configuration that reaches value up to 83.9%. The reason is that the air-gap structure not only weakens the surface-wave propagation but also promotes radiation by an improved mechanism.

The asymmetric dual air-gap design outperforms all the above-mentioned designs simultaneously in terms of gain, bandwidth and radiation efficiency with good matching. The aforementioned results confirm that the proposed design offers an efficient, practical and economical solution for microstrip antennas with high performance, standing out both from size considerations as well as cost per unit area owing to the utilization of low-cost the FR-4 substrate.

Fabrication Tolerance Analysis: Small variations in the air-gap dimensions, substrate thickness, and patch alignment may slightly shift the resonant frequencies and affect the realized gain and impedance matching. Alternatively, an asymmetric dual air-gap design offers an acceptable performance due to its wide impedance bandwidth and stable VSWR characteristics against typical PCB fabrication conditions. Therefore, this type of structure is ideal for practical fabrication via traditional low-cost FR-4 processes.

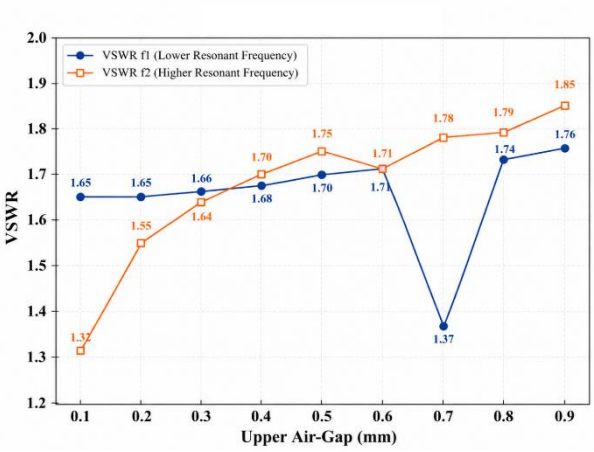

Figure 11: Variation of VSWR for both operating bands versus upper air-gap height.

Surface Current Distribution Analysis

To gain further insight into the physical mechanisms responsible for the performance improvement, the surface current distributions at different operating frequencies are analyzed, as shown in Figure 12.

In the baseline design, most of the current is concentrated at the feedline and in a small central region around the patch This indicates that a significant portion of the electromagnetic energy remains confined within the dielectric substrate, resulting in reduced radiation efficiency and increased dielectric losses.

In contrast, the proposed asymmetric dual air-gap design exhibits a stronger surface current distribution along the edges of the radiating patch at 4.953 GHz. Such behavior represents effective radiation and attenuated surface-wave propagation.

On the other hand, at a higher frequency (i.e., 8.146 GHz), the current distribution indicates that higher-order modes are excited to achieve dual-band operation.

These observations strongly support the theoretical analysis presented in Section 3.2, confirming that the proposed air-gap structure effectively suppresses surface-wave propagation while improving radiation efficiency.

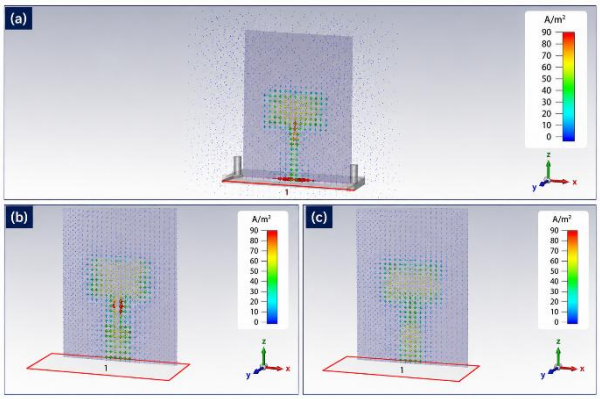

Figure 12: Surface current distribution on the proposed antenna with varying antenna configurations: (a) baseline design at 4744 MHz, (b) asymmetric dual air-gap configuration at 4953 MHz and (c) asymmetric dual air-gap configuration at 8146 MHz.

Radiation Patterns and Polarization

The proposed antenna is evaluated for near- and far-field radiation patterns at the dominant resonance frequency. Fig. 13 shows normalized radiation patterns in the E-plane and H-plane.

The findings reveal that antenna directionality is consistent with well-defined mainlobe signalling regions, making it suitable for practical wireless communication applications

This indicates that the HPBW is balanced in both planes. Moreover, the cross-polarization level in the broadside direction is kept lower than −15 dB, showing good polarization purity.

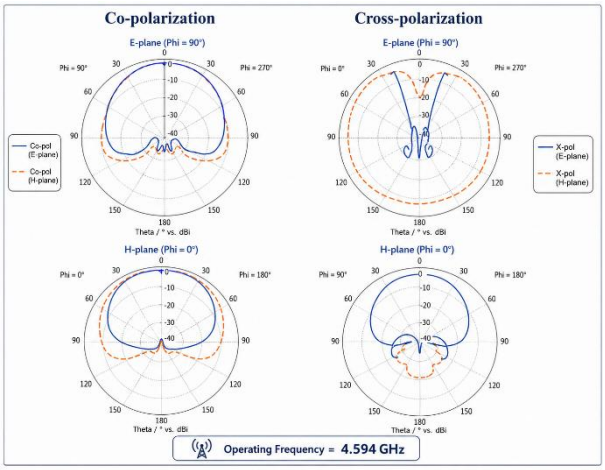

Figure 13: Normalized simulated radiation patterns at 4.9 GHz for (a) E plane and (b) H plane.

Comparison with Existing Works

Table 4 presents a comparison between the proposed antenna and recently reported designs employing various gain-enhancement techniques, such as defected ground structures (DGS), meta surface-based superstrates, dual-layer meta surface configurations and reconfigurable meta surface antennas.

The proposed antenna achieves a realized gain of 9.05 dBi at 4.95 GHz while maintaining excellent impedance matching (VSWR < 1.8) and high radiation efficiency (83.9%).

Conventional gain-enhancement techniques based on defected ground structures (DGS) generally provide only moderate gain improvement because they mainly modify the ground-current distribution without significantly increasing the effective radiating aperture(12).

Meta surface-based antennas(10, 11) play readily with the radiated field's phase distribution to realize higher gain levels. Configured as a dielectric superstrate, this geometry achieves gain enhancements of up to 10.3 dB by forming a partially reflective surface that improves the field collimation found in ordinary antennas(24). In a similar note, the dual-layer meta surface proposed in(25) results in gain levels of 7.5–9.3 dB by carefully managing electromagnetic coupling and minimizing phase mismatch between radiating elements.

The gain can also be improved dynamically with advanced designs like that of the reconfigurable meta surface antenna in(26) wherein, using electromagnetic device characterization, the designed structure has a gain of 11.1 dB. Such designs,

however, often need additional biasing circuits and complex control methods to work at the intended output level, significantly increasing system complexity as well as overall cost and power consumption.

The radiation gain of the proposed antenna based on an asymmetric dual air-gap configuration is 9.05 dB; this value is higher than traditional designs that implement DGS (12)and comparable to state-of-the-art structures based on meta surfaces(24, 26). Two principal physical mechanisms contribute to this performance enhancement.

First, more importantly, layers of air gap are included to decrease effectively the permittivity of the substrate structure, help increase foregone electromagnetic fields along patch edges and hence contribute to high radiation efficiency. This decreases the effective permittivity of this structure and causes the effective electrical size of the radiating element as well to grow while its physical dimensions remain constant, thus resulting in higher antenna gain and better radiation characteristics. The range of ε_eff is reduced as a result of the above, which increases the effective electrical size of the radiating element and enhances radiation characteristics without increasing the physical sizes.

Second, the asymmetric dual air-gap structure increases electromagnetic coupling between the radiating patch and ground plane and obtains more uniform surface current distribution for better radiation performance. This controlled coupling also lowers the Q-factor, enhancing impedance bandwidth and stabilizing the VSWR response.

Compared with metasurface-based designs, the proposed antenna does not depend on extra dielectric layers, periodic structures or active components. As a result, it has a fairly basic geometry, is less complicated to manufacture, and is cheaper. Additionally, in comparison with the reconfigurable antennas, biasing networks and control circuits are not required for this design, improving their applicability in practical implementations.

In summary, the introduced antenna concept is a simple and effective solution to achieve gain improvement, radiation efficiency, simplicity of structure and ease of fabrication. Although metasurface or reconfigurable techniques provide solutions with higher gain values, the proposed design can yield a comparable performance level with orders of magnitude reduced complexity such that it is also a potential solution in practical wireless communication systems.

Table 4: Comparison of the proposed antenna performance with existing literature.

Ref.	Frequency (GHz)	Gain (dBi)	Technique
(12)	5.8	5.10	Rectangular patch antenna with Defected Ground Structure (DGS)
(24)	5.19 – 6.26	10.3	Meta surface-based patch antenna with dielectric superstrate
(25)	4.7 – 6.66	7.5 – 9.3	Dual-layer meta surface patch antenna
(26)	5.1	11.1	Meta surface-based reconfigurable patch antenna
This Work	**4.95**	**9.05**	**Asymmetric dual air-gap patch antenna (proposed design)**

Conclusion

In this study, a high-performance microstrip patch antenna based on an asymmetric dual air-gap configuration has been proposed and investigated. While the concept offers significant advantages, it is limited for large-power applications because of intrinsic properties of low-cost the FR-4 substrates including high dielectric losses and surface-wave excitation.

The results demonstrate that incorporating air-gap layers reduces the effective permittivity of the antenna structure, leading to a significant improvement in radiation efficiency and suppression of surface-wave propagation. In particular, the asymmetric dual air-gap configuration provides additional design flexibility for controlling the electromagnetic coupling and resonance characteristics, resulting in further performance enhancement.

The peak realized gain and radiation efficiency are up to 9.05 dBi and 83.9% for the proposed antenna, while those of conventional FR-4 antenna are 3.38 dBi and about 36–46%, respectively. This configuration provides improved radiation performance while maintaining low fabrication complexity and cost.

Furthermore, the proposed antenna exhibits dual-band operation at 4.953 GHz and 8.146 GHz with an impedance bandwidth of approximately 526 MHz in the upper operating band. These results demonstrate that the asymmetric dual air-gap configuration is an effective method to reduce Q-factor with corresponding improvement in bandwidth performance.

Furthermore, the surface-current analysis confirms that the proposed configuration effectively suppresses surface-wave propagation while enhancing radiation efficiency, in agreement with the theoretical analysis.

Hence, the proposed antenna overcomes the challenges associated with low-performance FR-4 microstrip antennas and serves as a practical (inexpensive) solution for sub-6 GHz and X-band wireless communication systems.

Disclosure Statement

Ethics approval and consent to participate

Not applicable. This study is based entirely on numerical simulations using CST Microwave Studio and does not involve human participants, animals, or clinical data.

Consent for publication

Not applicable.

Availability of data and materials

The datasets generated and/or analyzed during the current study are available from the corresponding author upon reasonable request.

Author Contributions

Muayyed Jabar Zoory conceived and designed the study, performed the antenna modeling and simulations, analyzed the results, and prepared the original manuscript draft. Sarah Mohammed contributed to data interpretation, manuscript review, editing, and validation of the results. Both authors reviewed and approved the final version of the manuscript.

Funding

The authors received no financial support for the research, authorship, and/or publication of this article.

Research Source Statement

This manuscript is based on research conducted as part of an ongoing Master's thesis at Mustansiriyah University. The thesis has not yet been completed, submitted, or published.

Conflicts of interest

The authors declare that they have no known competing financial interests or personal relationships that could have appeared to influence the work reported in this paper.

Acknowledgements

The authors would like to extend their thanks to Mustansiriyah University (www.uomustansiriyah.edu.iq) for their great support in the current work.

References

1] Balanis CA. Antenna theory: analysis and design. 4th ed. Hoboken (NJ): John Wiley & Sons; 2016. https://www.wiley.com/en-us/Antenna+Theory:+Analysis+and+Design,+4th+Edition-p-9781118642061

2] Pozar DM. Microstrip antennas. Proceedings of the IEEE. 1992;80(1):79–91. https://doi.org/10.1109/5.119568

3] Riaz A, Khan S, Arslan T. Design and modelling of graphene-based flexible 5G antenna for next-generation wearable head imaging systems. Micromachines. 2023;14(3):610. https://doi.org/10.3390/mi14030610

4] Mohammed AJ, Zoory MJ, Mohamad HJ. Study the effect of slotting microstrip antennas by theoretical simulations for Ka-band applications. AIP Conference Proceedings. 2026. https://doi.org/10.1063/5.0330459

5] Garg R, Bhartia P, Bahl IJ, Ittipiboon A. Microstrip antenna design handbook. Norwood (MA): Artech House; 2001. Available from: https://books.google.com/books?id=_er1LO5pEnUC

6] Mohammed SK, Zoory MJ. Design and experimental validation of a high-efficiency FR-4 microstrip patch antenna based on a single air-gap configuration for wireless applications. Journal of Theoretical and Applied Physics. 2026. https://doi.org/10.57647/jtap.2026.2005.02

7] Jaafar H, Ali MT, Subahri S, Yusof AL, Salleh MKM. Improving gain performance by using air substrate at 5.8 GHz. In: 2012 International Conference on Computer and Communication Engineering (ICCCE); 2012. https://doi.org/10.1109/ICCCE.2012.6271159

8] . Al Kharusi KWS, Ramli N, Khan S, Ali MT, Halim MA. Gain enhancement of rectangular microstrip patch antenna using air gap at 2.4 GHz. International Journal of Nanoelectronics and Materials. 2020;13(Special Issue):211-224. Available from: https://ijneam.unimap.edu.my/

9] Noor SK, Jusoh M, Sabapathy T, Rambe AH, Vettikalladi H, Albishi AM, et al. A patch antenna with enhanced gain and bandwidth for sub-6 GHz and sub-7 GHz 5G wireless applications. Electronics. 2023;12(12):2555. https://doi.org/10.3390/electronics12122555

10] Jung JI, Yang JR. 5.8-GHz patch antenna with an enhanced defected ground structure for size reduction and increased bandwidth. Journal of Electromagnetic Engineering and Science. 2022;22(3):245-251. https://doi.org/10.26866/jees.2022.3.r.83

11] Yang F, Rahmat-Samii Y. Microstrip antennas integrated with electromagnetic band-gap (EBG) structures: A low mutual coupling design for array applications. IEEE Transactions on Antennas and Propagation. 2003;51(10):2936-2946. https://doi.org/10.1109/TAP.2003.817983

12] Hasan MN, Rana MS. Gain enhanced 5.8 GHz patch antenna with defected ground structure: design and measurement. TELKOMNIKA (Telecommunication Computing Electronics and Control). 2025;23(5):1147-1154. https://doi.org/10.12928/TELKOMNIKA.v23i5.26755

13] Arrak HA, Zoory MJ, Rahi SK. Improving the performance of microstrip patch antennas by air gap and array configurations: A design and analysis investigation at 2.4 GHz. AIP Conference Proceedings. 2026. https://doi.org/10.1063/5.0328070

14] Supreeyatitikul N, Janpangngern P, Lertwiriyaprapa T, Krairiksh M, Phongcharoenpanich C. CMA-based quadruple-cluster leaf-shaped metasurface-based wideband circularly polarized stacked-patch antenna array for sub-6 GHz 5G applications. IEEE Access. 2023;11:14511-14523. https://doi.org/10.1109/ACCESS.2023.3244119

15] Holloway CL, Kuester EF, Gordon JA, O'Hara J, Booth J, Smith DR. An overview of the theory and applications of metasurfaces: The two-dimensional equivalents of metamaterials. IEEE Antennas and Propagation Magazine. 2012;54(2):10-35. https://doi.org/10.1109/MAP.2012.6230714

16] Fakharian MM, Rezaei P, Azadi A, Dadras M. A capacitive fed microstrip patch antenna with air gap for wideband applications. International Journal of Engineering, Transactions B: Applications. 2014;27(5):715-722. Available from: https://www.ije.ir/article_72581.html

17] Nikolic MM, Djordjevic AR, Nehorai A. Microstrip antennas with suppressed radiation in horizontal directions and reduced coupling. IEEE Transactions on Antennas and Propagation. 2005;53(11):3469-3476. https://doi.org/10.1109/TAP.2005.858847

18] Arrak HA, Zoory MJ, Rahi SK. Design and optimization of multi-substrate microstrip patch antennas for enhanced gain and return loss performance at 2.4 GHz. AIP Conference Proceedings. 2026. https://doi.org/10.1063/5.0328060

19] Waterhouse RB. Broadband stacked shorted patch. Electronics Letters. 1999;35(2):98-100. https://doi.org/10.1049/el:19990086

20] Ollikainen J, Fischer M, Vainikainen P. Thin dual-resonant stacked shorted patch antenna for mobile communications. Electronics Letters. 1999;35(6):437-438. https://doi.org/10.1049/el:19990324

21] James JR, Hall PS, editors. Handbook of microstrip antennas. London: Institution of Engineering and Technology; 1989. Available from: https://digital-library.theiet.org/content/books/ew/pbew028e

22] Wong KL. Compact and broadband microstrip antennas. New York: John Wiley & Sons; 2002.

Available from: https://www.wiley.com/en-us/Compact+and+Broadband+Microstrip+Antennas-p-9780471417172
23] Anguera J, Font G, Puente C, Borja C, Soler J. Multifrequency microstrip patch antenna using multiple stacked elements. IEEE Microwave and Wireless Components Letters. 2003;13(3):123-124. https://doi.org/10.1109/LMWC.2003.810126
24] Budarapu SK, Sunder MS. Performance enhancement of patch antenna using meta surface and dielectric superstrate for 5GHz Wi-Fi applications. In: Second International Conference on Emerging Trends in Engineering (ICETE 2023). Dordrecht: Atlantis Press; 2023. p. 793-800. https://doi.org/10.2991/978-94-6463-252-1_96
25] Yang K, Wang M, Jia X. Improved bandwidth of patch antenna using dual-layer metasurface. Progress In Electromagnetics Research Letters. 2025;124:69-75. https://doi.org/10.2528/PIERL24120601
26] Elias BQ, Ismail MM, Bashar BS, Alanssari AI, Rhazali Z, Misran H. Multi-beam metasurface control based on frequency reconfigurable antenna. Informacije MIDEM. 2024;54(2):77-85. https://doi.org/10.33180/InfMIDEM2024.201